

MICROCOPY RESOLUTION TEST CHART
NATIONAL BUREAU OF STANDARDS-1963-A

R00-924428-1

12
A

LEVEL

ELECTRON-BEAM-SUSTAINED BLUE/GREEN LASER PUMP

ADA081423

Prepared by
R.T. Brown and W.L. Nighan

Final Technical Report
February 1980

DTIC
ELECTE
S MAR 4 1980 D
A

Sponsored by the Naval Ocean Systems Center
under Contract N00014-78-C-0830

**UNITED TECHNOLOGIES
RESEARCH CENTER**



DISTRIBUTION STATEMENT A
Approved for public release
Distribution Unlimited

UNITED TECHNOLOGIES

EAST HARTFORD, CONNECTICUT 06108

DDC FILE COPY

80 3 3 124

00-00-100-1

Unclassified

SECURITY CLASSIFICATION OF THIS PAGE (When Data Entered)

REPORT DOCUMENTATION PAGE		READ INSTRUCTIONS BEFORE COMPLETING FORM
1. REPORT NUMBER R80-924428-1	2. GOVT ACCESSION NO.	3. RECIPIENT'S CATALOG NUMBER 9
4. TITLE (and Subtitle) 6 Electron-Beam-Sustained Blue/Green Laser Pump.	5. PERFORMING ORG. REPORT NUMBER 14 UTRC R80-924428-1	6. DATE OF REPORT (and Period Covered) Final Technical Report. Sep 1978 — Feb 1980
7. AUTHOR(s) 10 R. T. Brown and W. L. Nighan	8. CONTRACT OR GRANT NUMBER(s) 15 N00014-78-C-0830	
9. PERFORMING ORGANIZATION NAME AND ADDRESS United Technologies Research Center Silver Lane East Hartford, Connecticut 06108	10. PROGRAM ELEMENT, PROJECT, TASK AREA & WORK UNIT NUMBERS	
11. CONTROLLING OFFICE NAME AND ADDRESS Director, Physics Program Office of Naval Research 800 North Quincy Street, Arlington VA 22217	11. REPORT DATE Feb 1980	
14. MONITORING AGENCY NAME & ADDRESS (if different from Controlling Office) 12 46	13. NUMBER OF PAGES 44	15. SECURITY CLASS. (of this report) Unclassified
16. DISTRIBUTION STATEMENT (of this Report) Approved for public release; distribution unlimited. Reproduction in whole or in part is permitted for any purpose of the United States Government.		15a. DECLASSIFICATION/DOWNGRADING SCHEDULE
17. DISTRIBUTION STATEMENT (of the abstract entered in Block 20, if different from Report)		
18. SUPPLEMENTARY NOTES		
19. KEY WORDS (Continue on reverse side if necessary and identify by block number) Excimer laser, KrF* laser, XeCl* laser, Electron-beam controlled electric discharge XeCl* laser		
20. ABSTRACT (Continue on reverse side if necessary and identify by block number) Techniques are described for prolonging the duration of stable e-beam controlled excimer laser discharges, including: temporal tailoring of either the discharge voltage or the ionization source, and kinetics modification by way of additives. Theoretical and experimental results are presented for KrF* laser discharges. → next page		

DD FORM 1 JAN 73 1473

EDITION OF 1 NOV 68 IS OBSOLETE
S/N 0102-LF-014-6601

Unclassified

SECURITY CLASSIFICATION OF THIS PAGE (When Data Entered)

409252

gw

Unclassified

SECURITY CLASSIFICATION OF THIS PAGE(When Data Entered)

Block 20

XeCl(B) formation processes are examined for conditions typical of a discharge excited laser using HCl as the chlorine donor. It is shown that vibrational excitation of HCl followed by dissociative attachment is a primary step in the reaction sequence resulting in Cl^{\leftarrow} . XeCl(B) formation is the result of a three-body $\text{Xe}^{\leftarrow} - \text{Cl}^{\leftarrow}$ recombination reaction. Experimental results are presented which demonstrate efficient (~ 2%) XeCl laser operation in an e-beam assisted discharge in which over 75% of the energy was deposited by the discharge.

about

Unclassified

SECURITY CLASSIFICATION OF THIS PAGE(When Data Entered)

R80-924428-1

ELECTRON-BEAM-SUSTAINED BLUE/GREEN LASER PUMP

TABLE OF CONTENTS

	<u>Page</u>
1. INTRODUCTION	1
2. KrF* STUDIES	4
A. Experimental Facilities	4
B. Theoretical and Experimental Results	5
3. XeCl* STUDIES	11
A. Background	11
B. Kinetic Modeling Studies	11
C. E-Beam Assisted Discharge Experiments	16
D. Discussion	19
 REFERENCES	
APPENDIX 1 - STABILITY ENHANCEMENT IN ELECTRON-BEAM SUSTAINED EXCIMER LASER DISCHARGES	 A-1

1. INTRODUCTION

One of the critical requirements for the Navy Strategic Blue/Green Optical Communications Programs is a blue/green laser with a high pulse energy, with high repetition-rate capability, and with a long operational lifetime. A leading candidate for such a laser is the XeCl*(B → X) laser, frequency shifted from 308 nm into the blue/green spectral range. Recent studies (Ref. 1) demonstrated XeCl* electrical-optical conversion efficiencies in the 5 percent range and showed superior long-life performance when HCl was used as the halogen donor. Furthermore, efficient (up to 50 percent) conversion efficiency has been demonstrated (Ref. 2) for frequency shifting the XeCl* laser output into the blue/green spectral region using Raman conversion in metal vapors.

Under the present contract United Technologies Research Center (UTRC) has carried out an investigation of an electron-beam-sustained XeCl* laser for use as the pump source for such a Raman shifted blue/green laser (Ref. 3). The objective of the UTRC program has been to demonstrate technology which will provide the basis for a long-life electron beam sustained XeCl* discharge laser for Navy blue/green applications.

Major accomplishments under the present contract include:

- Successful demonstration of UTRC devised techniques to enhance the stability, energy loading and discharge: e-beam energy ratio of e-beam sustained excimer laser discharges.
- Identification of vibrational excitation of HCl as a fundamental process in the XeCl(B) formation sequence.

- Identification of Xe^+-Cl^- recombination as the XeCl(B) formation process in discharge excited XeCl lasers.
- Development of an e-beam assisted discharge design permitting attainment of large volume, long duration, diffuse XeCl discharges having properties compatible with Navy requirements.

The initial phase of the present program dealt primarily with techniques for enhancing the stability of an e-beam sustained discharge, and utilized the well understood KrF^* laser system at 248 nm as a means of demonstrating the physical principles involved (Ref. 4). These stability enhancement techniques were originally developed under UTRC Corporate sponsorship, and were conceived as a means of developing discharge technology which would achieve the volumetric scalability and high efficiency of pure e-beam pumping, but which would require significantly lower e-beam current densities than those typically utilized for pure e-beam pumping (Ref. 5). Under the present contract, the UTRC stability enhancement techniques were successfully reduced to practice in a manner which exceeded original expectations. Specific details of this portion of the present investigation are described in Section 2.

While the KrF^* laser results demonstrated the viability of the UTRC approach, it was realized at the outset that the problems of closed cycle chemistry and the lack of an efficient frequency conversion technique for 248 nm radiation probably preclude use of the KrF^* laser for Navy blue/green applications. Therefore, under the second phase of the present program, emphasis has been placed on the XeCl^* laser operating with Ne/Xe/HCl mixtures. Operation with this mixture has

shown high efficiency (Ref. 1) with a significant reduction in the problems related to closed cycle laser chemistry (Ref. 6). As will be discussed in Section 3, the kinetic processes in Ne/Xe/HCl mixtures are significantly different from those in Ar/Kr/F₂ mixtures, thereby precluding a direct application of tailoring techniques discussed in Ref. 4 to the XeCl discharge. However, the technology base developed in the KrF studies has allowed rapid progress with the XeCl system, with the results being the attainment of good XeCl laser properties at low e-beam current densities and with high discharge enhancement factors. These results are presented in Section 3 and demonstrate efficient (~ 2 percent) XeCl laser operation in an e-beam assisted discharge in which over 75 percent of the energy was deposited by the discharge.

2. KrF* STUDIES

A. Experimental Facilities

Experiments were carried out using a 1.5 cm x 2 cm x 50 cm active volume under conditions typical of those corresponding to optimum KrF* laser operation.

Discharge pulse length could be varied for times up to 1.0 μ sec. Great care was taken in designing the experiment so as to maximize spatial and temporal uniformity of the discharge electric field and of the electron-beam power deposition. The electron beam was produced by a cold-cathode diode operated with a nearly constant 300 kV, 1 μ sec pulse, and a slowly increasing current pulse. A scale diagram of the e-beam system is shown in Fig. 2-1. The discharge cell was constructed using stainless steel, aluminum, and Kynar; Viton O-rings were used throughout. A flat stainless-steel screen was used as the discharge cathode and the anode was a Rogowski-profiled aluminum electrode located 1.5 cm from the cathode. The electron beam window was an unsupported 1 mil titanium foil 1.5 cm x 50 cm in cross-section located 0.64 cm behind the discharge cathode screen. A diagram of the discharge chamber is shown in Fig. 2-2, and a photograph of the chamber is shown in Fig. 2-3. A photograph of the overall experimental arrangement is shown in Fig. 2-4.

For the KrF experiments, the discharge voltage was supplied by a low-inductance capacitor circuit and was coupled into the discharge via a strip-line. Experimental diagnostics included measurements of the electron-beam voltage and current, discharge voltage and current, discharge fluorescence intensity, and time integrated photographs of the discharge volume. Total discharge current was measured by monitoring the voltage drop across a series resistor and the discharge voltage was measured using

a low inductance voltage divider connected directly across the discharge electrodes. The KrF* fluorescence at 248.5 nm was monitored using a fast photodetector (< 5 nsec risetime) with a narrow-band (8 nm half-width) filter centered at 248 nm.

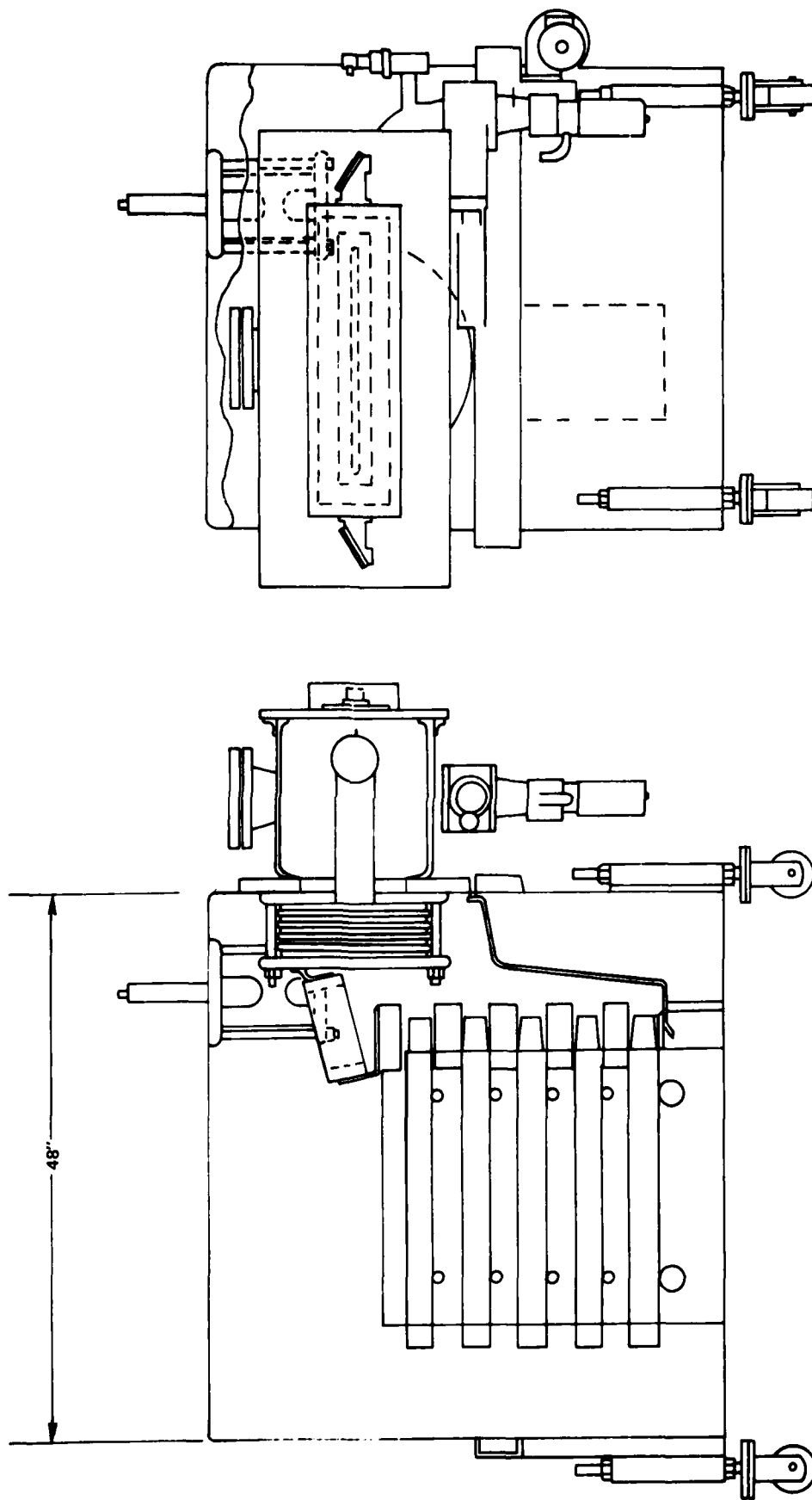
Prior to carrying out discharge experiments a number of tests were performed in order to characterize the electron beam. The diode voltage was monitored using an ammonium chloride voltage divider probe and the total diode current was monitored using a B-dot loop. The electron-beam intensity was measured using both rose cinemoid film and a small scanning Faraday cup, and was found to be uniform along the 50 cm dimension to within ± 5 percent. Measurements in air at 1 atm, and at a distance 2 cm from the foil window, showed that the transverse beam intensity profile was nearly Gaussian, with a half-width of 2.0 cm. In addition, measurements were made in argon at 1 atm with a 1 cm diameter Faraday cup placed 0.7 cm from the discharge cathode screen. These measurements showed that the current density increased linearly by approximately 50 percent during the 1 μ sec pulse, and showed small (± 15 percent) fluctuations on a fast time scale (< 50 nsec). The measured current density in argon was used to estimate the local electron-beam power deposition by using tabulated stopping powers (Ref. 13) increased by a factor of 2.5 to account for multiple scattering effects (Ref. 14).

B. Theoretical and Experimental Results

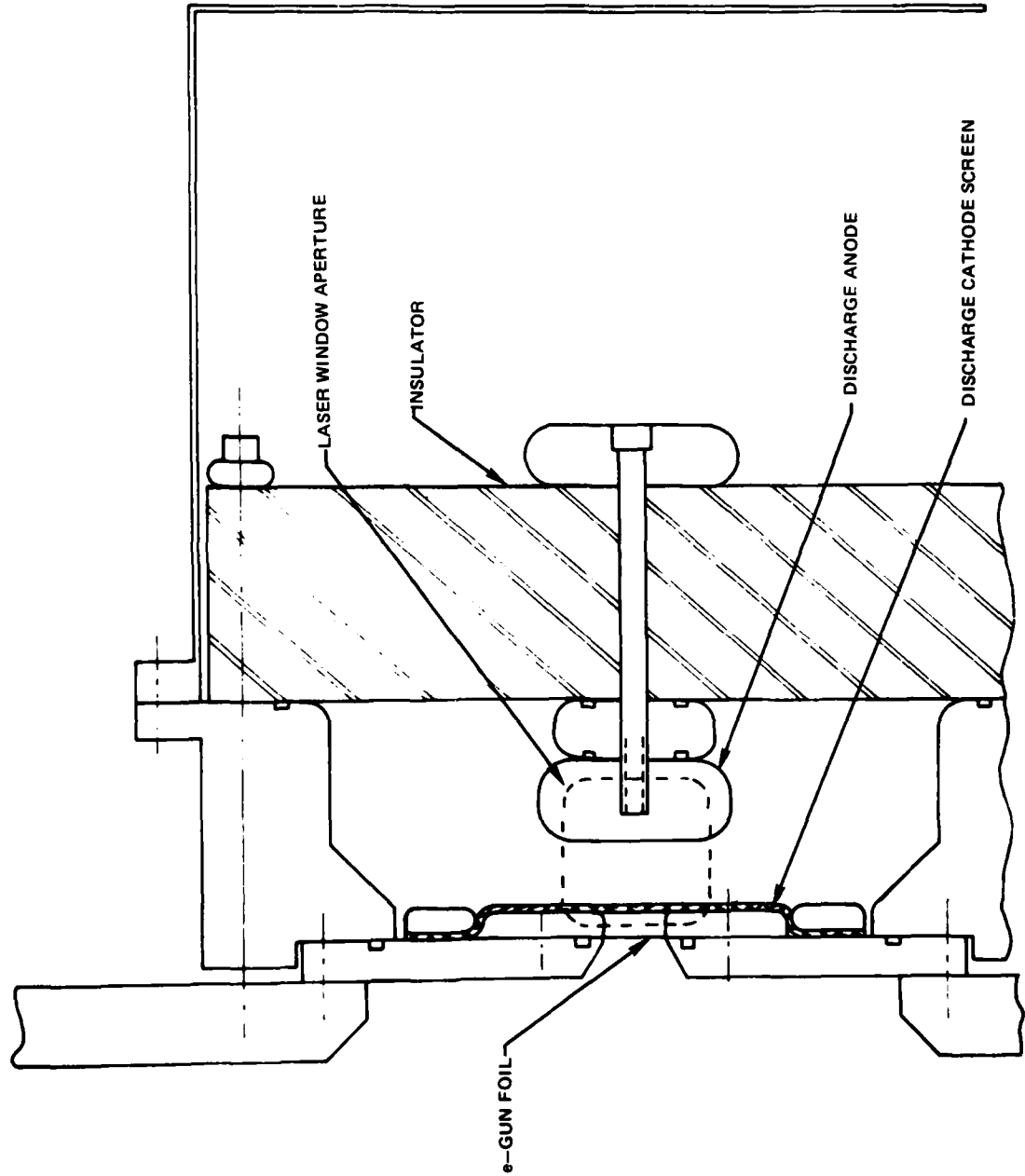
The stability enhancement techniques considered in the present study involved either temporal tailoring of the discharge voltage, temporal tailoring of the electron-beam current density, or use of halogen mixtures. Specific details of this portion of the investigation are described in detail in Ref. 4, which is

included herein as Appendix 1. As discussed in Ref. 4, an essential feature of the stability enhancement techniques is the fact that for discharges in Ar/Kr/F₂ mixtures, typical of optimum KrF laser mixtures, a stable e-beam sustained discharge regime exists for which KrF* production by way of the Kr* metastable channel is very efficient (Ref. 5). For the voltage tailoring approach, a second requirement is that the discharge impedance be high, so that circuit impedance effects can be minimized and so that a well controlled voltage pulse shape can be obtained. For KrF mixtures, this was found to be the case.

SCALE DIAGRAM OF ELECTRON BEAM SYSTEM



CROSS SECTION OF e-BEAM-SUSTAINED DISCHARGE CHAMBER



ELECTRON BEAM SUSTAINED DISCHARGE CELL



ELECTRON-BEAM SUSTAINED DISCHARGE EXPERIMENT



78 01 203 5
78 10 A

3. XeCl* STUDIES

A. Background

While the KrF* laser results demonstrated the viability of the UTRC approach, it was recognized at the outset that the problems of closed cycle chemistry and the lack of an efficient frequency conversion technique for 248 nm radiation probably preclude use of the KrF* laser for Navy blue/green applications. Therefore, under the second phase of the present program, emphasis has been placed on the XeCl* laser operating with Ne/Xe/HCl mixtures. Operation with this mixture has shown high efficiency (Ref. 1) with a significant reduction in the problems related to closed cycle laser chemistry (Ref. 6). However, as will be discussed below, the kinetic processes in the Ne/Xe/HCl laser mixture are significantly different from those in the KrF* laser mixture, a circumstance precluding a direct application of the tailoring techniques discussed above to the XeCl discharge. Nonetheless, the technology base developed in the KrF portion of the investigation has allowed rapid progress with the XeCl system, with the result being the attainment of good XeCl laser properties at low e-beam current densities ($\sim 1 \text{ A/cm}^2$) and with high discharge energy enhancement factors (~ 10).

B. Kinetic Modeling Studies

In spite of the prior demonstration of high efficiency with the XeCl/HCl laser (Ref. 1), at the time the present XeCl program was initiated, relatively little was known about HCl reaction kinetics in the XeCl laser medium. The following paragraphs discuss certain specific aspects of this problem, and present the findings of

our investigation of XeCl(B) formation kinetics and plasma processes in the UTRC electron-beam assisted discharge.

There are several important features which set HCl apart from other effective halogen donors: (1) a high dissociation energy (4.45 eV); (2) a very high cross-section for vibrational excitation by electrons (Ref. 7); and (3) a cross-section for dissociative attachment from the ground vibrational level which is substantially lower than that of the halogen donors typically used in rare-gas fluoride lasers. Formation of XeCl(B) by way of $\text{Xe}(^3\text{P}_2)\text{-HCl}$ reactions is slightly endothermic at 300°K (Ref. 8), reflecting the strong HCl bond energy. Thus, the large measured (Ref. 8) $\text{Xe}(^3\text{P}_2)$ quenching rate by HCl is apparently a purely dissociative reaction and does not result in formation of the XeCl(B) upper laser level. Although quenching of $\text{Xe}(^3\text{P}_1, ^3\text{P}_0, ^1\text{P}_1)$ by HCl may result in XeCl(B) formation, at present there are no data for such reactions. In addition, while the large cross-section for HCl vibrational excitation ensures the presence of a high fractional concentration of vibrationally excited HCl in laser plasmas, there is no evidence suggesting efficient XeCl(B) formation by way of $\text{Xe}(^3\text{P}_2)\text{-HCl}(v)$ reactions.

On the basis of these considerations it was concluded that a more likely consequence of HCl vibrational excitation is enhanced dissociative attachment. Indeed, our analysis of current-voltage characteristics for the electron-beam controlled discharges in a variety of rare-gas-HCl mixtures indicates the occurrence of an electron loss process which increases with time throughout the discharge pulse. Modeling studies show that this enhanced electron loss correlates with the growth in the concentration of vibrationally excited HCl. Further,

without taking this effect into account, it is not possible to quantitatively model either discharge characteristics or laser properties in XeCl laser mixtures on the basis of other known reactions alone.

Presented in Fig. 3-1 are the rate coefficients for vibrational excitation and attachment for HCl in the ground vibrational level, computed for a Ne(.989)-Xe(.01)-HCl(.001) laser mixture. The vibrational cross-section of Rohr and Linder (Ref. 7) was used in the calculation, and the shape of the attachment cross-section of Ziesel, Nenner, and Shultz (Ref. 9) was used, adjusted in magnitude to yield a rate coefficient consistent with our experimental observations in vibrationally cold HCl. The shaded region in this figure is indicative of the ten-to-twenty fold increase in the effective attachment rate of HCl resulting from vibrational excitation, as deduced from the present modeling of the characteristics of rare-gas HCl discharges. Very recent measurements by Wong (Ref. 10) indicate more than an order of magnitude increase in the attachment cross-section due to HCl vibrational excitation, a result that provides additional support to the present conclusions.

On the basis of the interpretation discussed above, it is concluded that vibrational excitation of HCl is a fundamental process in XeCl lasers using HCl as the chlorine donor. For discharge excited lasers, modeling studies indicate that XeCl(B) formation proceeds by way of the sequence illustrated in Fig. 3-2. In this sequence, electron energy transfer is dominated by Xe metastable production and by excitation of metastable atoms to the higher lying manifold of Xe p states. Production of Xe^+ is found to be a cumulative process in which stepwise ionization of

metastable and p state atoms make comparable contributions. Formation of XeCl(B) results from the three-body recombination of Xe^+ with Cl^- , the latter produced by dissociative attachment to vibrationally excited HCl as discussed previously. Of course, there are numerous energy loss processes interfering with the simplified XeCl(B) formation sequence illustrated in Fig. 3-2, particularly electron elastic collisions with Ne, $Xe(p \rightarrow s)$ relaxation by neutral collisions, and dissociative quenching of both Xe metastable and p state atoms by HCl. Even under optimum laser discharge conditions, these loss processes account for approximately 50 percent of the discharge energy. Nevertheless, numerical analysis shows that XeCl(B) is produced according to the sequence indicated in Fig. 3-2 with an efficiency in the 5-10 percent range for a wide range of discharge conditions.

As indicated in Fig. 3-2, a major conclusion of our kinetic analyses to date is that XeCl(B) formation proceeds by way of an ionization-recombination channel, and that XeCl(B) formation by way of the Xe^* metastable channel is negligible. This is in sharp contrast to KrF, for which the dominant formation process in an e-beam sustained discharge is by way of the Kr^* metastable level (Ref. 5). Formation of XeCl(B) only by way of the ion channel has significant implications regarding both the stability of an e-beam sustained XeCl discharge and the role of the e-beam. Since the objective of the e-beam sustained discharge approach is to supply the majority of the input energy with the discharge field rather than with the e-beam, when the upper laser level is formed by way of ionization-recombination reactions as in the XeCl laser, it is necessary that the discharge supply the majority of the ionization as well. Thus, in contrast to KrF, there

is no efficient operating regime in which the Xe^+ ionization is provided primarily by the external source, with the input energy provided by the discharge electric field. The XeCl discharge must therefore operate in a quasi-avalanche mode, and in fact must operate in an unstable regime (Ref. 11). Under such circumstances the discharge is e-beam "assisted" rather than e-beam "sustained" as is the case with KrF.

C. E-Beam Assisted Discharge Experiments

A major accomplishment of the UTRC program during the past year has been the development and testing of an e-beam assisted discharge design having the potential for scaling to large volume, long duration, diffuse XeCl laser discharges. In the present investigation, the e-beam discharge arrangement described in Section 2 was utilized with an active discharge volume of 1.5 cm x 2.0 cm x 50 cm. For the reasons discussed in the previous section, during the initial phase of the experimental program, the kinetic modeling of the XeCl discharge had not yet been developed to the predictive capability stage. Thus, a semi-empirical approach to the initial experiments was required. As a starting point, the gas mixtures and pressures of Ref. 1 were used, and the e-beam current density was set to a value comparable to that used for the KrF studies. Initial experiments were carried out with a discharge driving circuit which had been designed for use with KrF mixtures. These tests showed that for a given electron beam source intensity the electron density in the XeCl mixture was much higher than in typical KrF mixtures, with a correspondingly lower discharge impedance. While

these early results were dominated by circuit inductance and resistance effects, the tests demonstrated diffuse, long-time (600 nsec) discharge pulses and correspondingly long-time laser pulses at 308 nm.

In order to improve the coupling efficiency between the discharge driver and the discharge, a close-coupled circuit with a series inductance of ~ 35 nh and a series resistance (used as a current viewing resistor) of 0.01Ω was constructed. In order to eliminate the inductance and lifetime problems associated with series switching, this circuit was operated in a mode in which the e-beam assisted discharge was self-switched; i.e., the discharge charging voltage was below the self-breakdown voltage prior to the initiation of the electron beam. A diagram of this very simple circuit is shown in Fig. 3-3. Initial tests with this circuit showed a number of trends: (1) The XeCl discharge impedance was typically two orders of magnitude less than that for KrF discharges. (2) The XeCl* fluorescence efficiency increased with E/n. (3) The attainable discharge: e-beam energy enhancement factor was limited by the onset of constricted arcs in the discharge. (4) Under typical conditions, the e-beam provided only a small fraction of the total ionization.

Throughout these tests, correlations were made with analytical studies in order to better understand the trends and to determine which parameter changes were likely to yield the greatest improvements in performance. As discussed in Section 2, it became apparent that operation in the quasi-avalanche mode was an essential feature of efficient operation of the e-beam assisted XeCl discharge. Thus, much of the experimental emphasis was placed on developing discharge driver

designs and discharge electrode designs which would allow operation in the unstable mode, but which at the same time could operate with good impedance matching and without constricted arcing.

In carrying out the experiments, a typical procedure was to vary the value of the electron beam source (maintained constant during the pulse), and to vary the values of the driving capacitance and the initial charging voltage until a set of conditions were found which yielded a pulse duration in the 200-350 nsec range, a good impedance match, and a good intrinsic electrical-optical conversion efficiency. Since the e-beam system in these experiments was a research-oriented facility, only a small fraction (less than 0.1 percent) of the electrical input energy to the e-beam system was actually deposited in the discharge volume. Therefore, the efficiency and enhancement factor were calculated based on deposited energy, as discussed in Section 2, rather than on total electrical input energy.

Figure 3-4 shows representative current-voltage characteristics for the laser mixture of Fig. 3-1 at a total pressure of 3 atmospheres. The discharge was triggered by initiation of a 0.5 μ sec electron-beam pulse at a current density level of 2 Acm^{-2} . Following initiation of the e-beam pulse, the applied voltage collapsed from an initial level of approximately $4.5 \times 10^{-17} \text{ Vcm}^2$ to a value of about $1.9 \times 10^{-17} \text{ Vcm}^2$. The total energy deposited by the discharge in this case was 6.4 J and the energy deposited by the electron beam was 1.1 J, corresponding to a discharge; e-beam energy enhancement factor of 6. As shown in Fig. 3-4, the onset of the $\text{XeCl}(B \rightarrow X)$ laser pulse occurred approximately 0.15 μ sec after the

initiation of the discharge current pulse and lasted for 0.35 μsec . Measured laser pulse energy was 0.16 J corresponding to an intrinsic electrical-optical energy conversion efficiency of about 2 percent; while measured values of peak gain for these conditions were about 3.1 percent cm^{-1} . For the e-beam levels and cavity parameters of this experiment, laser oscillation due to the e-beam alone was near the threshold level and often was not discernable at all.

Typical numerical results corresponding to the conditions of Fig. 3-4 are shown in Fig. 3-5, in which small-signal gain, small signal absorption, XeCl(B) formation efficiency, and discharge: e-beam energy enhancement factor are plotted versus time. The UTRC code used for these calculations incorporates the effective attachment rates discussed in Section 2, and uses best estimates of rates for which detailed data are not presently available. As would be expected, the temporal profiles of these properties were found to be very sensitive to the initial electron density and to the E/n temporal profile used as input for the calculation. For the results shown in Fig. 3-5, input values typical of experimental values were used. For the conditions of Fig. 3-5, the calculated volumetric absorption was dominated by Xe_2^+ , and to a lesser extent by Ne_2^+ and Cl^- , and was at a level approximately one tenth that of the gain, consistent with an optical extraction efficiency of about 40 percent. On this basis, the computed XeCl(B) formation efficiency of 4.5 percent is in satisfactory agreement with the measured laser efficiency (formation efficiency times extraction efficiency) of 2.0 percent. The computed gain is also in accord with the experimental observation. For the conditions of Fig. 3-4, the laser burn pattern

essentially imaged the discharge cross-section, indicating that the gain was quite uniform over the 1.5 cm x 1.8 cm optical aperture used in these experiments. The results in Figs. 3-4 and 3-5 are very significant since they demonstrate that the e-beam assisted discharge approach allows the attainment of large-volume, long-duration, diffuse XeCl discharges, even when the discharge is operated in the unstable regime required for efficient XeCl(B) production.

In carrying out tests with the low inductance circuit, it became clear that cathode phenomena had an important effect on the onset of arcing in the discharge. For this reason, considerable emphasis was placed on developing an optimized cathode design. The best results to date were obtained with a very fine-mesh etched metal screen cathode, a Rogowski-profiled aluminum anode, and with the e-beam passing through the cathode screen. Results obtained with this electrode arrangement and with an optimally matched discharge circuit are shown in Fig. 3-6. The results in Fig. 3-6 represent a significant improvement over the results in Fig. 3-5, obtained with an earlier cathode design. In Fig. 3-6 the required e-beam current density was 0.8 A cm^{-2} , compared to 2.0 A cm^{-2} in Fig. 3-5.

D. Discussion

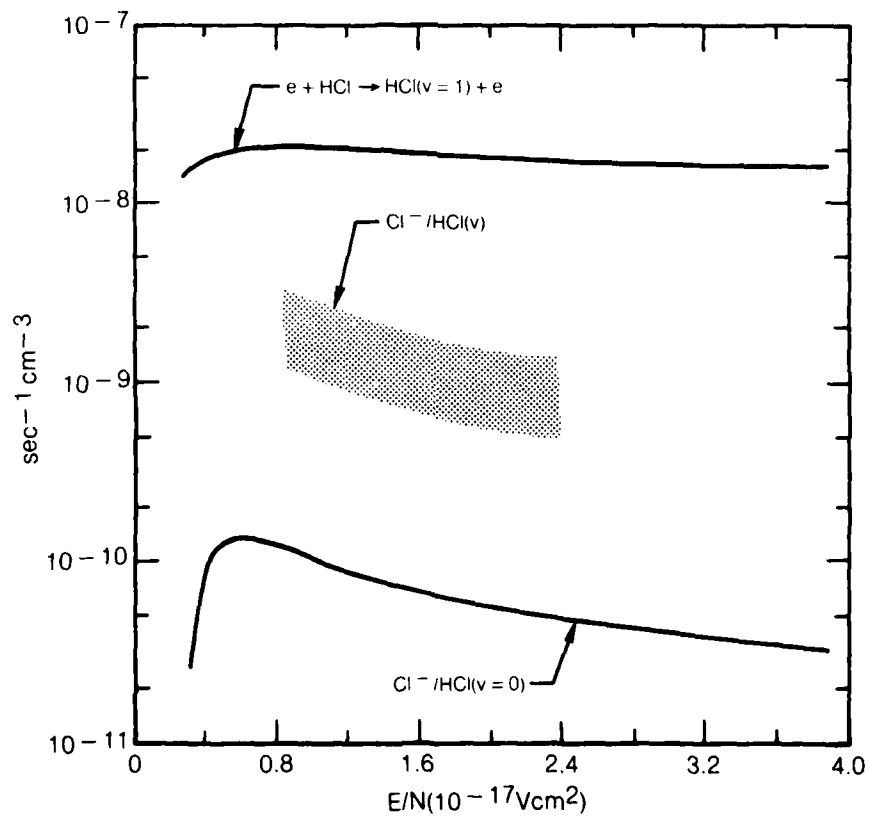
As mentioned earlier, the long-term objective of the present program is to develop an XeCl laser with an output pulse energy in excess of 2 J and with the capability of operating at high repetition rates for very long times. The results described above are a major step toward this goal for the following reasons: (1) The discharge excitation process appears to be volumetrically scalable, allowing the design of an efficient XeCl laser of arbitrarily large pulse

energy (e.g., up to 20 J) simply by increasing the active volume. (2) The discharge driving circuit for the UTRC approach is extremely simple and utilizes components which are compatible with high-rep-rate, long life operation. (3) The low e-beam current densities characteristic of the e-beam assisted approach are compatible with efficient, high-rep-rate, long-life operation of an e-beam system.

In order to move from the present small-scale, XeCl studies to a system capable of meeting Navy requirements, there are four technology issues which must be addressed: (1) Volumetric scale-up of the discharge cell, including e-beam window foil, discharge electrodes, and laser optics; (2) Scale-up of the discharge driver; (3) Development of a closed-cycle gas flow system, including the incorporation of materials and subsystems necessary for eliminating long-term chemistry problems; and (4) Development of an efficient e-beam system, with capabilities matched to the full-scale e-beam assisted XeCl discharge, and with high-rep-rate, long-life capability. Based on the results of the present study, it appears that these technology problems can be solved and that a closed-cycle e-beam assisted XeCl laser will be capable of meeting the requirements of the Navy Strategic Blue/Green Optical Communications Program.

**RATE COEFFICIENTS FOR VIBRATIONAL EXCITATION AND DISSOCIATIVE ATTACHMENT
FOR HCl IN THE GROUND VIBRATIONAL LEVEL**

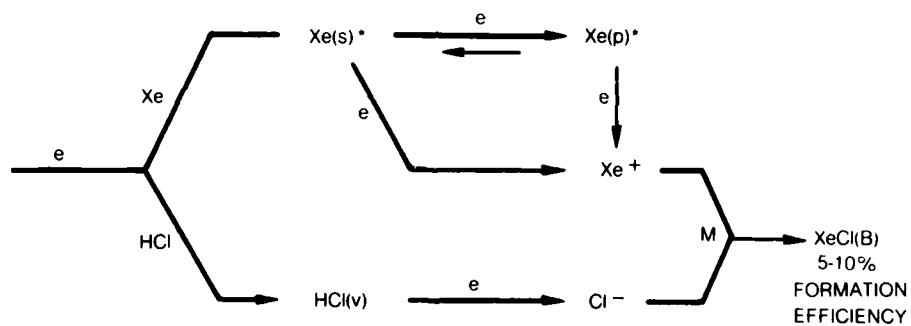
Ne/Xe/HCl = 0.989/0.01/0.001



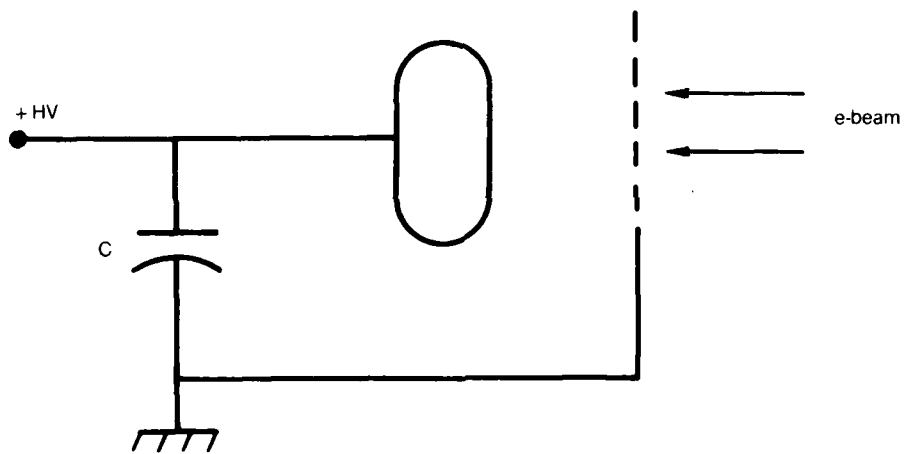
1.5 2.0 2.5

MEAN ELECTRON ENERGY eV

**XeCl(B) FORMATION SEQUENCE IN DISCHARGE EXCITED
Ne — Xe — HCl LASER MIXTURES**

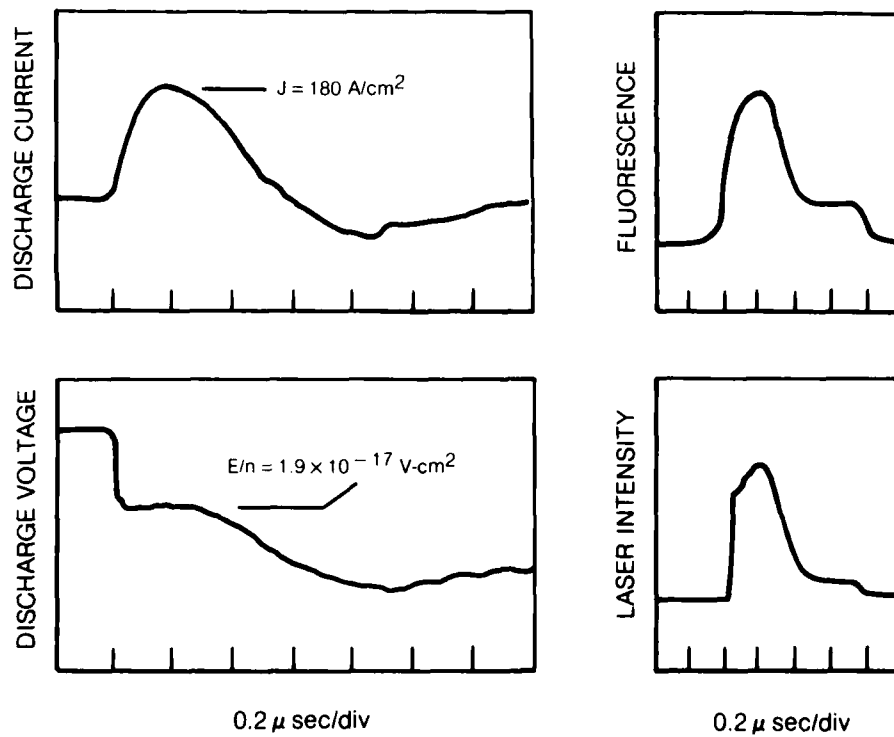


DISCHARGE DRIVING CIRCUIT



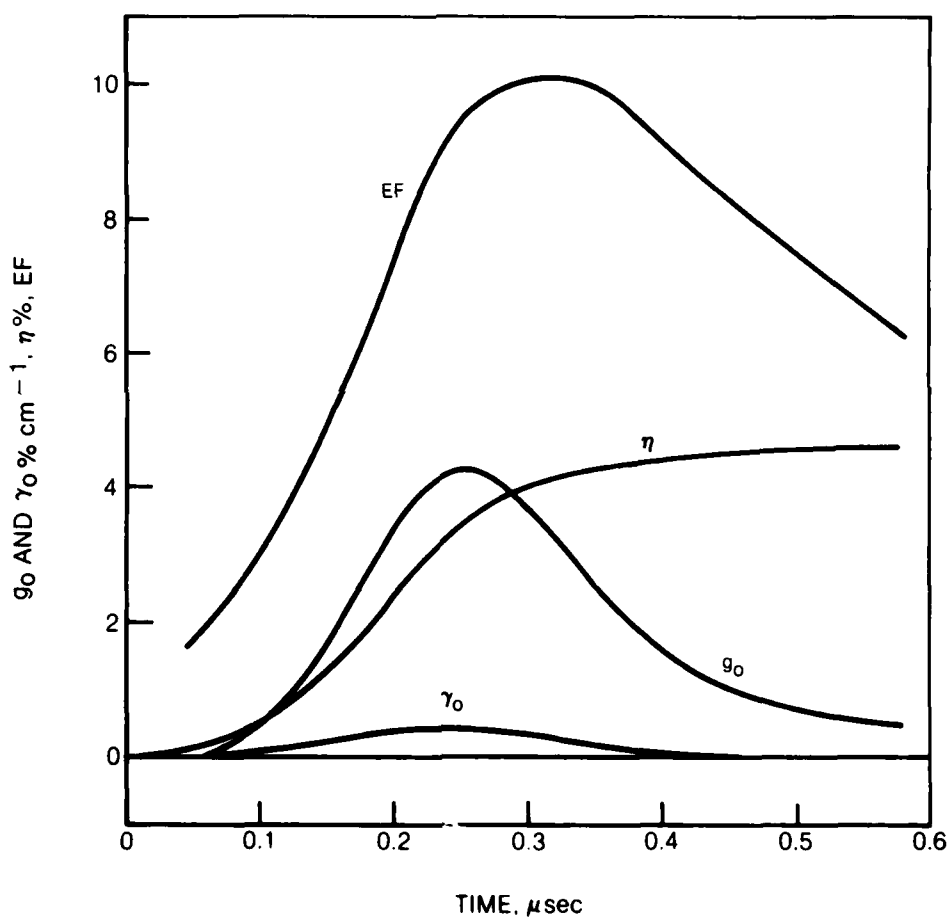
**MEASURED CHARACTERISTICS IN AN E-BEAM ASSISTED
XeCl LASER DISCHARGE**

Ne/Xe/HCl = 0.989/0.01/0.001
 $p = 3 \text{ atm}$ $J_e = 2.0 \text{ A/cm}^2$
WIRE SCREEN CATHODE



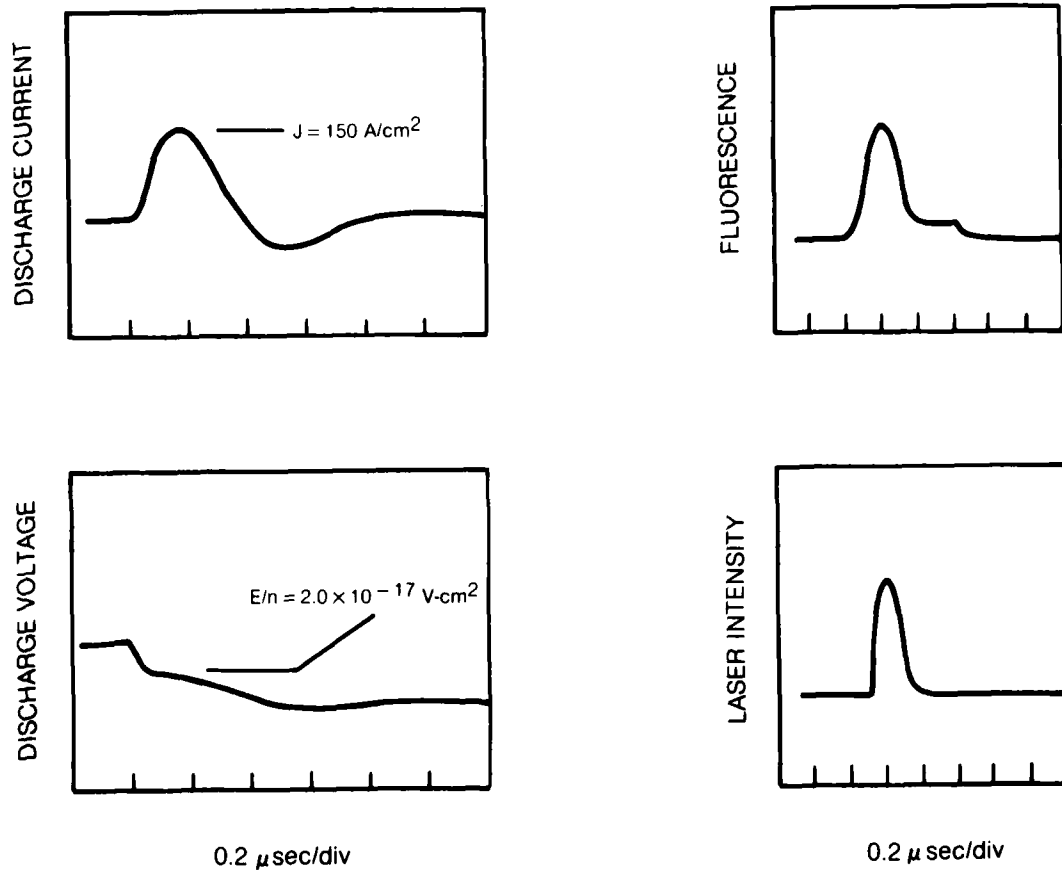
CALCULATED XeCl LASER PROPERTIES

Ne/Xe/HCl = 0.989/0.01/0.001; p = 3 atm



**MEASURED CHARACTERISTICS IN AN E-BEAM ASSISTED
XeCl LASER DISCHARGE**

Ne/Xe/HCl = 0.989/0.01/0.001
 $p = 3 \text{ atm}$ $j_e = 0.8 \text{ A/cm}^2$
ETCHED SCREEN CATHODE



REFERENCES

1. Champagne, L. F.: Efficient Operation of the Electron-Beam Pumped XeCl Laser. *Appl. Phys. Lett.*, 33, p. 523, 1978.
2. Burnham, R. and N. Djeu: Efficient Raman Conversion of XeCl Laser Radiation in Metal Vapors. (To be published).
3. Nighan, W. L. and R. T. Brown: Efficient XeCl(B) Formation in An Electron-Beam Assisted Xe/HCl Laser Discharge. (*Applied Physics Letters*; in press).
4. Brown, R. T. and W. L. Nighan: Stability Enhancement in Electron-Beam Sustained Excimer Laser Discharges. *Appl. Phys. Lett.*, 35, p. 142, 1979, (Appendix 1).
5. Brau, Ch. A.: Rare Gas Halogen Excimers. In *Excimer Lasers*, Ch. K. Rhodes, Ed., Springer-Verlag, Ch. 4, p. 87, New York, 1979
6. Miller, J. L., J. Dickie, J. Davin, J. Swingle, and T. Kan: Operating Characteristics of a Closed Cycle Flow Rare Gas Halide Laser. *Appl. Phys. Lett.*, 35, p. 912, 1979.
7. Rohr, K. and F. Linder: Vibrational Excitation of Polar Molecules by Electron Impact I Threshold Resonances in HF and HCl. *J. Phys. B: Atom. Molec. Phys.* 9, p. 2521, 1976.
8. Koltz, J. H., J. E. Velazco and D. W. Setser: Reative Quenching Studies of Xe($6S, ^3P_2$) Metastable Atoms by Chlorine Containing Molecules. *J. Chem. Phys.* 71, p. 1247, 1979.
9. Ziesel, J. P., I. Nenner, and G. J. Schulz; Negative Ion Formation, Vibrational Excitation, and Transmission Spectroscopy in Hydrogen Halides. *J. Chem. Phys.* 63, p. 1943, 1975.
10. Wong, S. F: Recent Trends in Beam Experiments on Dissociative Attachment. Symposium on Electron-Molecule Collisions, U. of Tokyo, September 1979, Invited Papers, Eds. I. Shimamura and M. Matsuzawa.
11. Daugherty, J. D., J. A. Mangano and J. H. Jacob: Attachment-Dominated Electron-Beam-Ionized Discharges. *Appl. Phys. Lett.*, 28, p. 581, 1976.
12. Brown, R. T. and W. L. Nighan: Instability Onset in Electron-Beam-Sustained KrF Laser Discharges. *Appl. Phys. Lett.*, 32, p. 730, 1978.

REFERENCES (Cont'd)

13. Berger, M. J., and S. M. Seltzer: Tables of Energy-Losses and Ranges of Electrons and Positrons. Studies of Penetration of Charged Particles in Matter, National Academy of Science Pub., 1133, Chap. 10, 1967.
14. Hart, G. A. and S. K. Searles: Kinetic Model of the XeBr Rare-Gas Monohalide Excimer Laser. J. Appl. Phys. 47, 2033 (1976).

APPENDIX A

Stability Enhancement in Electron-Beam Sustained

Excimer Laser Discharges*

by

Robert T. Brown and William L. Nighan

United Technologies Research Center

East Hartford, CT 06108

ABSTRACT

Techniques are described for prolonging the duration of stable e-beam controlled excimer laser discharges, including: temporal tailoring of either the discharge voltage or the ionization source, and kinetics modification by way of additives. Theoretical and experimental results are presented for KrF* laser discharges.

For practical, high-power excimer laser systems, it is desirable to utilize electron-beam sustained discharge excitation rather than electron-beam excitation alone, since for a given laser output power the burden on the electron-beam technology is significantly lower. One of the major obstacles to implementing the e-beam-sustained discharge technique is the onset of ionization instability.¹⁻³ In this paper a number of techniques for improving excimer laser discharge stability are outlined and theoretical and experimental results are presented for an electron-beam sustained KrF* laser discharge.

It has been shown^{2,3} that the major factor contributing to instability in electron-beam controlled KrF* laser discharges is dissociation of the molecular halogen, F₂, during the discharge pulse. This can be readily appreciated upon examination of the following approximate expression¹⁻³ for the instability growth rate, ν , i.e.,

$$\nu \approx 2n^* k_i - n_{F_2} k_a \quad (1)$$

where n^* and n_{F_2} are the number densities of rare-gas metastable atoms and fluorine molecules, while k_i^* and k_a are the rate coefficients for metastable ionization and electron dissociative attachment, respectively. For conditions typical of KrF* laser mixtures,³ the electron conservation equation is well approximated by the relation,

$$nS \approx n_e n_{F_2} k_a \quad (2)$$

and the metastable conservation equation can be approximated by,

$$n_e n k_{ex}(E/n) \approx n^* n_{F_2} k_a \quad (3)$$

where n is the density of ground state rare-gas atoms, S is the ionization rate due to the electron beam, $k_{ex}(E/n)$ is the metastable production rate coefficient (exhibiting a very strong E/n dependence³), and k_Q is the rate coefficient for loss of metastables due to F_2 quenching. Combination of Eqs. 1-3 yields the following criterion for discharge stability (i.e., $\nu < 0$),

$$\frac{2n^2 k_i^+ S k_{ex}(E/n)}{n_{F_2}^3 k_0^2 k_Q} < 1 \quad (4)$$

For the parameter values required for efficient rare-gas halide laser operation it has been shown³ that the left side of this inequality is usually in the 0.1-0.5 range, indicative of a marginally stable situation.

In most e-beam controlled KrF* lasers the discharge E/n value is typically maintained at a relatively constant level throughout the pulse, while the e-beam source function (S) tends to increase due to the space-charge limited mode of operation of cold-cathode e-beam guns. This tendency results in an increase in the numerator on the left side of inequality (4), i.e., reduced stability. More importantly, the form of (4) indicates that the onset of instability ($\nu \geq 0$) is exceptionally sensitive to the dissociative loss of F_2 . Since F_2 dissociation is primarily a consequence of rare gas-halide formation itself,³ invariably a point in time is reached for which electron density disturbances are amplified, i.e., inequality (4) is violated and the discharge becomes unstable. At the high values of E/n (i.e., higher values of k_{ex}) required for effective discharge energy enhancement and high discharge power density, the unstable point is reached earlier in the pulse.^{2,3}

The form of the stability criterion (4) discussed above suggests several techniques for increasing the stable duration of the discharge pulse while

maintaining laser properties near their optimum values. These include: (1) temporal tailoring of either the discharge voltage (E/n), i.e., controlled temporal reduction of k_{ex} , or of the e-beam ionization source function, S , in order to compensate for F_2 loss; and (2) modification of the halogen kinetics in such a way that loss of F_2 has a less severe effect on the occurrence of instability.

The stabilizing influence of judicious temporal reduction in either S or k_{ex} (i.e., E/n) in order to compensate for the changes in plasma properties caused by the dissociative loss of F_2 is conceptually straightforward. The potential role of halogen kinetics modification is best understood by observing that in conventional KrF* mixtures reactions involving F_2 control both the electron density (Eq. 2) and the metastable density (Eq. 3), a circumstance leading to the cubic dependence on F_2 concentration exhibited by inequality (4). This situation can be favorably altered by use of a two-component halogen mixture in which one species tends to dominate electron loss, while the other (the halogen fuel) dominates metastable processes and therefore excimer formation. Such is the case in certain F_2 - NF_3 mixtures, for example. The rate coefficient for electron dissociative attachment in NF_3 is approximately four times larger than that of F_2 , while the NF_3 -rare gas metastable atom quenching coefficient is about six times smaller than that of F_2 . Thus, addition of a relatively small amount of NF_3 ($NF_3/F_2 \leq 0.1$) to the conventional KrF* laser mixture will significantly affect the electron density but should exert little or no influence on other processes. Enhanced stability should result as a consequence of the weakened coupling between the electron and metastable concentrations.

Indeed, with NF_3 controlling the electron loss and F_2 the metastable loss, it is easily shown that the criterion for stability becomes,

$$\frac{2n^2 k_i^* S k_{ex}(E/n)}{n_{\text{F}_2} k_0 (n_{\text{NF}_3} k_0)^2} < 1 \quad (5)$$

Since dissociative NF_3 -metastable reactions will proceed at a much slower rate than the corresponding F_2 reactions, the impact of dissociation on electron density growth (plasma stability) should be lessened substantially as indicated by the linear dependence of (5) on F_2 concentration. Furthermore, use of NF_3 , an acceptable fluorine donor itself, does not introduce processes unfavorable to the efficient formation of KrF^* .

Detailed numerical evaluation of the stability enhancement techniques described above has been carried out using a comprehensive computer model of an e-beam controlled KrF^* laser discharge.³ Representative results are presented in Fig. 1 which shows the characteristic temporal runaway of the discharge current density indicative of ionization instability onset (curve (a)).¹ For curve (a) E/n was maintained at a constant value of $1.4 \times 10^{-16} \text{ Vcm}^2$, a condition for which instability onset occurs approximately $0.3 \mu\text{sec}$ after discharge initiation. Curve (b) illustrates the effect of a controlled linear reduction in E/n from an initial value of $1.4 \times 10^{-16} \text{ Vcm}^2$ to a value of approximately $1.0 \times 10^{-16} \text{ Vcm}^2$ after $1.0 \mu\text{sec}$. The predicted improvement in stability as reflected by the temporal variation in discharge current density is dramatic indeed, with the region of stable discharge behavior increasing to about $0.8 \mu\text{s}$, and the total energy deposited in the gas prior to the occurrence of instability increasing

by almost a factor of three. Moreover, the medium properties are sensibly uniform in time, having values compatible with efficient, high power laser operation⁴, e.g., KrF* production efficiency, 20%; zero-field gain, 2.5% cm⁻¹; gain: absorption ratio, 10; electric power density, 110 kWcm⁻³; and time integrated discharge energy enhancement, 5. Curve (c) illustrates the effect of NF₃ addition for an NF₃-F₂ concentration ratio of 0.1. The initially lower current density level reflects the increased attachment loss of electrons due the presence of NF₃. However, the improvement in discharge stability as measured by the temporal evolution of the current density is again readily apparent, with the computed energy deposited in the gas approximately twice as large as in the absence of NF₃ (curve (a)). In addition, average medium properties are comparable to those of curve (b). Numerous calculations carried out on the basis of a tailored e-beam ionization source, as well as a variety of combinations of the techniques outlined above, produced results generally similar to those of Fig. 1.

The stability enhancement techniques described above were investigated experimentally using an e-beam controlled discharge² having an active volume 1.5 cm x 2.0 cm x 50 cm. Presented in Fig. 2 are discharge current density, voltage, and KrF* fluorescence traces for an Ar(0.95)-Kr(0.05)-F₂(0.005) mixture at one atmosphere. The data of Fig. 2a correspond to a constant E/n value of 1.4 x 10⁻¹⁶ Vcm², and exhibit the onset of instability approximately 0.3 μsec after discharge initiation as indicated by the characteristic sharp rise in current density accompanied by a decrease in both voltage and KrF* fluorescence. The effect of discharge voltage tailoring was evaluated by changing the discharge driving capacitance from 0.9 μF to 0.5 μF which resulted in a nearly linear decrease in E/n from an initial value of 1.4 x 10⁻¹⁶ Vcm² in a manner similar to that

corresponding to curve (b) in Fig. 1. Figure 2b shows that, according to predictions, the onset of instability was delayed until about the 0.5 μsec point. The influence of NF_3 addition with constant E/n is represented by the data of Fig. 2c. The observed reduction in the initial current density level and the increase in stable discharge duration to about 0.7 μsec are also found to be in good agreement with analytical predictions.

Figure 3a shows that an increase in the constant E/n level to 1.8×10^{-16} Vcm^2 for the indicated Ar/Kr/ F_2 mixture resulted in instability onset in a time less than 0.1 μsec . However, upon introduction of 0.025% NF_3 ($\text{NF}_3/\text{F}_2 = 0.05$) and by reduction of the discharge driving capacitance from 10.0 μF to 0.25 μF in order to produce a temporal decrease in E/n , the stable pulse duration was increased to about 0.35 μsec . For these conditions the discharge power density was 117 kW cm^{-3} and the e-beam power deposition density was 16 kW cm^{-3} (corresponding to an e-beam current density of 2.0 A cm^{-2}). Thus, the discharge energy enhancement factor was about 7. Code calculations for these conditions indicate a zero-field gain of $3.4\% \text{ cm}^{-1}$, volumetric absorption of $0.2\% \text{ cm}^{-1}$, and KrF^* formation efficiency of 25%, values compatible with efficient, high-power laser operation⁴.

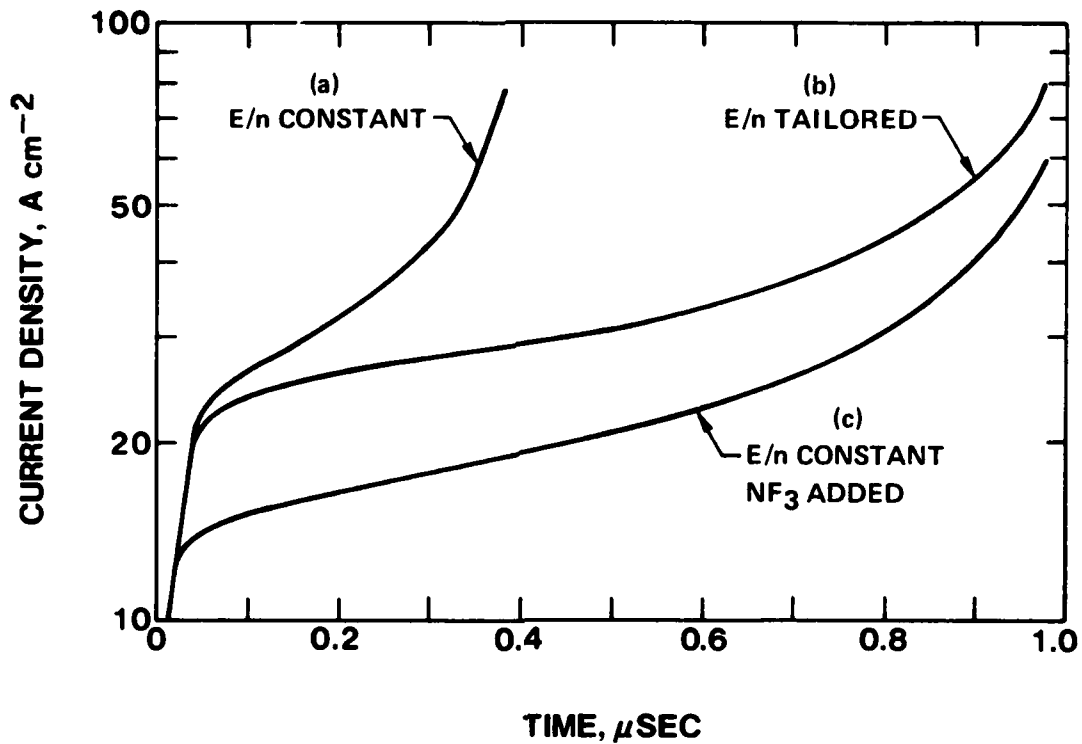
The stability enhancement techniques described herein are relatively simple to implement and offer the promise of efficient, scalable rare-gas halide and metal halide lasers at significantly reduced e-beam current density levels, thereby facilitating operation at high average power. At the present time a more complete reporting of this research is in preparation and work with other excimer lasers is underway.

The authors wish to thank Mr. R. Preisach for his excellent technical assistance with the experimental portion of the work.

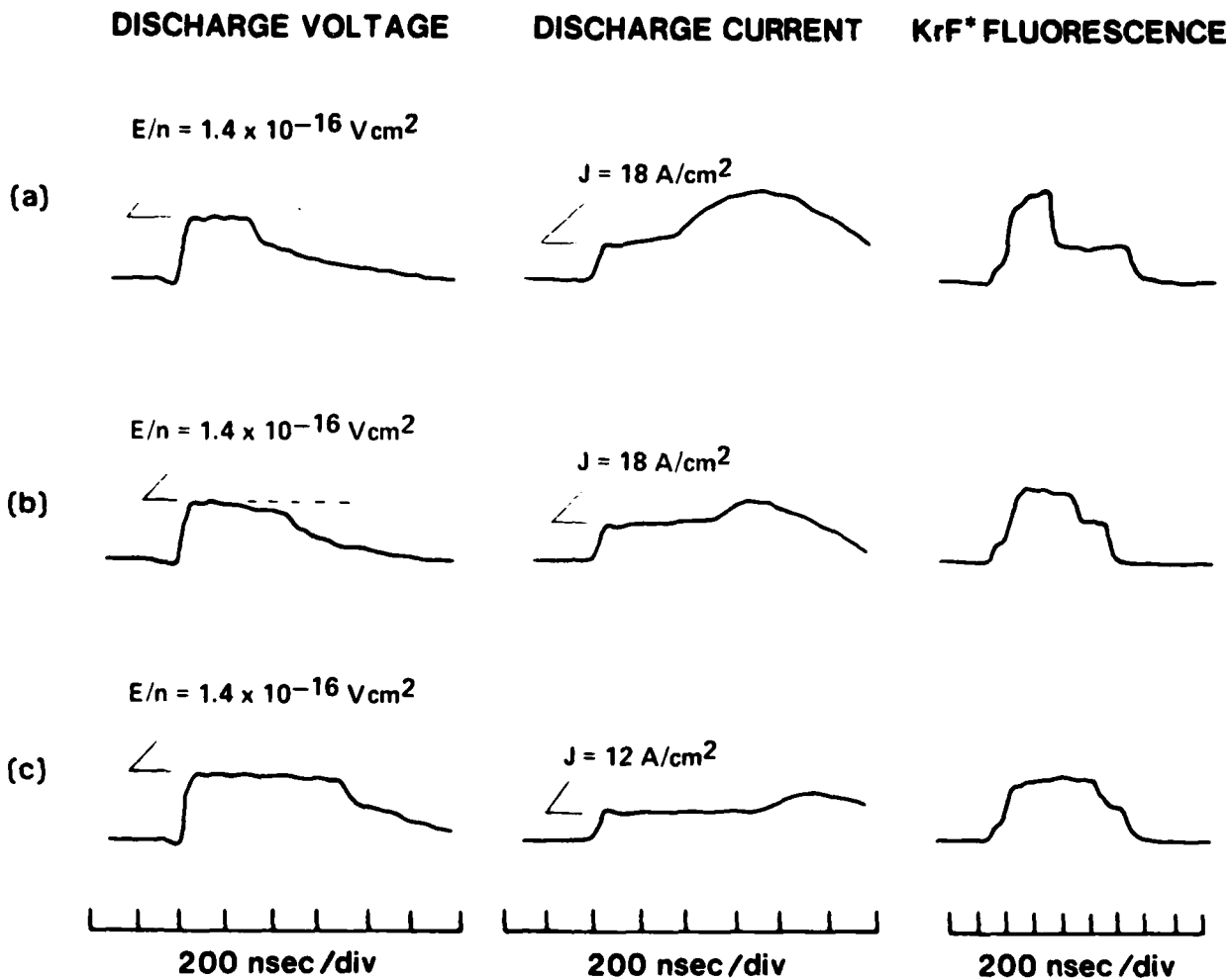
REFERENCES

* Supported in part by the Naval Ocean Systems Center and by the Office of Naval Research.

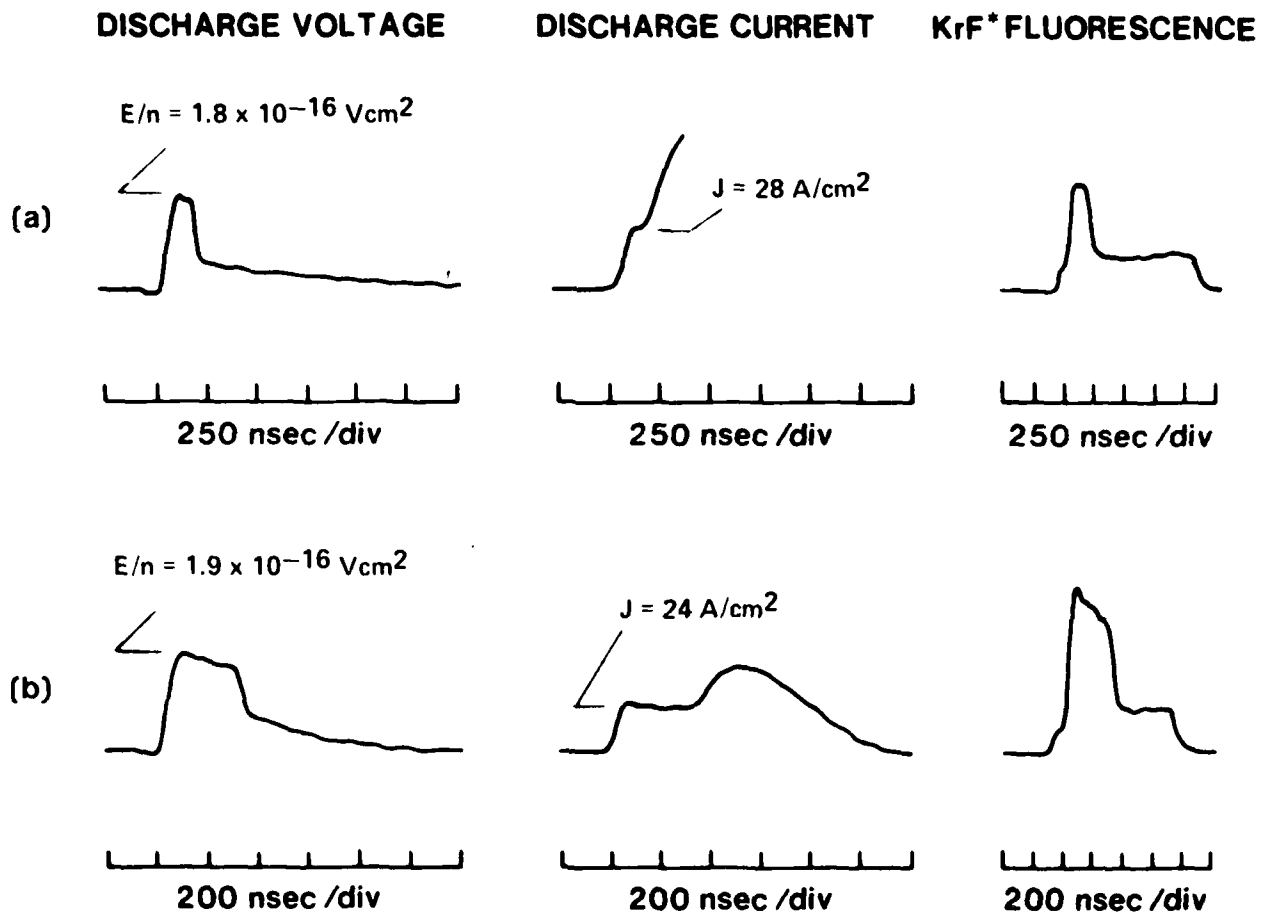
1. J. D. Daugherty, J. A. Mangano, and J. A. Jacob, Appl. Phys. Lett 28, 581 (1976).
2. R. T. Brown and W. L. Nighan, Appl. Phys. Lett. 32, 730 (1978).
3. W. L. Nighan, IEEE J. Quantum Electron. QE-19, 714(1978), and references cited therein.
4. M. Rokni, J. A. Mangano, J. H. Jacob, and J. C. Hsia, IEEE J. Quantum Electron QE-14, 464 (1978).



1. Computed current density profiles for an e-beam controlled Ar(0.95)-Kr(0.05)-F₂(0.005) mixture at one atmosphere. For each of these examples the initial E/n value was $1.4 \times 10^{-16} \text{ Vcm}^2$ and the e-beam ionization rate, S, was $150 + 7.5 \times 10^7 t \text{ sec}^{-1}$. (a) E/n constant; (b) E/n tailored according to the relation $1.4 \times 10^{-16} - 0.35 \times 10^{-10} t \text{ Vcm}^2$; (c) E/n constant with 0.05% NF₃ added.



2. Measured discharge characteristics for the mixture and e-beam ionization rate of Fig. 1. (a) E/n constant at $1.4 \times 10^{-16} \text{ Vcm}^2$; (b) capacitance of driving circuit reduced resulting in temporal reduction in E/n similar to that of curve b in Fig.1; (c) E/n constant at $1.4 \times 10^{-16} \text{ Vcm}^2$ with 0.05% NF_3 added.



3. Measured discharge characteristics for the mixture and e-beam ionization rate of Figs. 1 and 2. (a) E/n constant at $1.8 \times 10^{-16} \text{ Vcm}^2$; (b) temporal reduction in E/n from an initial value of $1.9 \times 10^{-16} \text{ Vcm}^2$ with 0.025% NF_3 added.

February 1980

Distribution List

Scientific Officer Director, Physics Program Physical Sciences Division Office of Naval Research 800 North Quincy Street Arlington, Virginia 22217 Attn: M. B. White - NR 395-592 Ref: Contract N 00014-78-C-0830	1 copy (with DD 250)
AF Plant Representative Off. (OL-AA, Det 4) AF Contract Mgt. Div. (AFSC) Pratt & Whitney Aircraft Group East Hartford, CT 06108 Attn: Mr. W. E. McAvoy ACO Code RBD	1 copy
Director, Naval Research Laboratory Attn: Code 2627 Washington, D.C. 20375 DODAAD Code N00173	6 copies
Defense Documentation Center Bldg. 5, Cameron Station Alexandria, Virginia 22314 DODAAD Code S47031	12 copies
Office of Naval Research Branch Office - Boston 666 Summer Street Boston, Mass. 02210 DODAAD Code N62879	1 copy
Dr. Kevin J. Kelley Code 8105 Naval Ocean Systems Center 271 Catalina Blvd. San Diego, CA 92152	1 copy

Distribution List (Cont'd)

Dr. E. J. Schimitschek Code 811 Naval Ocean Systems Center 271 Catalina Blvd. San Diego, CA 92152	1 copy
Dr. Robert E. Behringer Office of Naval Research 1030 East Green Street Pasadena, CA 91101	1 copy
Dr. R. Burnham Laser Physics Branch Naval Research Laboratory Washington, D.C. 20375	1 copy